LA-UR-19-23845 (Accepted Manuscript)

# Demonstration of transport of a patterned electron beam produced by diamond pyramid cathode in an rf gun

Nichols, Kimberley; Andrews, Heather Lynn; Kim, Dongsung; Simakov, Evgenya Ivanovna; Conde, Manoel; Doran, Darrell Scott; Ha, Gwanghui; Liu, Wanming; Power, John; Shao, Jiahang; Whiteford, Charles; Wisniewski, Eric E.; Antipov, Sergey; Chen, Gongxiaohui



**To be published in:** Applied Physics Letters

**DOI to publisher's version:** 10.1063/1.5128109

**Permalink to record:** http://permalink.lanl.gov/object/view?what=info:lanl-repo/lareport/LA-UR-19-23845

# Demonstration of Transport of a Patterned Electron Beam Produced by Diamond Pyramid Cathode in an rf Gun

K. E. Nichols,[1, a)] H. L. Andrews,[1] D. Kim,[1] E. I. Simakov,[1] M. Conde,[2] D. S. Doran,[2] G. Ha,[2] W. Liu,[2] J. F. Power,[2] J. Shao,[2] C. Whiteford,[2] E. E. Wisniewski,[2] S. P. Antipov,[3] and G. Chen[4]

[1)]*Los Alamos National Laboratory, Los Alamos, NM, 87544, USA*

[2)]*Argonne National Laboratory, Lemont, IL, 60439, USA*

[3)]*Euclid Beamlabs LLC, Bolingbrook, IL, 60440, USA*

[4)]*IIT, Chicago, IL, 60616, USA*

(Dated: 20 December 2019)

We have demonstrated generation and transport of a patterned electron beam from a Diamond Field-Emitter Array (DFEA) cathode in a radio-frequency (rf) gun. DFEAs are arrays of micron-scale pyramids with nanometer-scale tips. They can be fabricated with base widths ranging from 3 microns to 25 microns and pitches as small as 5 microns. They have an inherent 1:0.7 base to height ratio. DFEAs operate as field-emitter cathodes, and potentially produce intrinsically shaped electron beams, which are of interest for a number of accelerator applications. We report on the results of a recent experiment in which a beam, consisting of several beamlets, was produced from a DFEA cathode in an rf gun and transported 2.54 meters along a beam line. A macro-bunch charge of 60 pC was measured at a cathode field gradient of 15.1 MV/m.

Inherently shaped beams are advantageous for a variety of particle accelerator needs, such as reducing energy spread in the accelerating bunch due to beam loading[1,2] and production of ultra-short high current electron bunches[3]. One application that most benefits from an intrinsically shaped beam is the beam-driven collinear wakefield accelerators[4]. In this scheme a trailing low charge witness bunch is accelerated by a wakefield excited by a higher charge longitudinally shaped drive bunch traveling in the same structure or plasma medium[5,6]. A longitudinally shaped electron bunch can be produced directly a number of ways, however, these methods have limitations due to restricted response time of various electronic components and space charge effects. A method to produce longitudinally shaped electron bunches from a transversely shaped electron bunch by means of an emittance exchanger (EEX) has been proposed and demonstrated[7,8,9,10]. Another application of shaped beams is the production of temporally-shaped electron bunches at ultra-fast time scales for small footprint accelerator based light-sources[11].

A transversely shaped electron beam can be produced directly from a shaped cathode[12], by using a photocathode excited by a transversely shaped laser beam[13], or by the most popular method: use of a transverse mask to intercept a portion of the beam[9,8,10]. The disadvantages of the mask method include beam loss of up to 80%, production of hazardous x-rays, and inconsistent beam shapes shot-to-shot due to jitter. At Los Alamos National Laboratory we have proposed an alternative: to intrinsically produce transversely-shaped electron bunches from Diamond Field-Emitter Array (DFEA) cathodes[14,15].

DFEAs are arrays of diamond pyramids with exquisitely sharp tips as shown in Fig. 1. The pyramid arrays are fabricated using standard silicon wafer processing techniques so they can be fabricated in arbitrary shapes to produce an inherently shaped beam. DFEAs produce electron beams by field-emission with typical currents as high as 30 $\mu$A per pyramid at gradients of around 10 MV/m in the direct-current (dc) regime[16,17]. DFEAs emit under dc electric fields, as well as in time-varying electromagnetic fields in rf guns, as reported here. These cathodes can produce an inherently shaped beam with little to no current loss, no production of x-rays due to use of a mask, no shot-to-shot jitter, and no drive laser required.

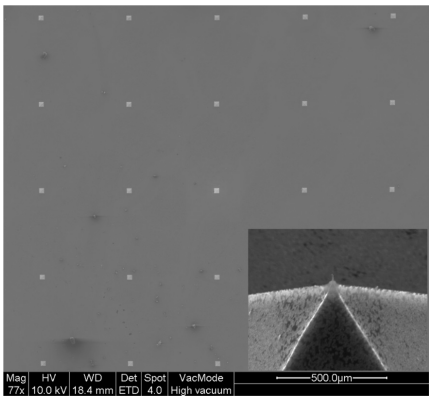


FIG. 1: An SEM image of a 5x5 array and close up of a single diamond tip (insert).

A field-emission cathode is of particular interest for use in an rf gun because it greatly simplifies the infrastructure needed to produce the beam, operates at lower fields, and is less expensive to implement and operate than photo cathodes. In addition, in an rf gun, field-emission cathodes will produce inherently shorter bunches with lower energy spread than thermionic cathodes[18]. For applications with relaxed beam quality requirements and stringent power/size requirements, field-emission cathodes such as DFEAs have many ad-

[a)]Electronic mail: knichols@lanl.gov.

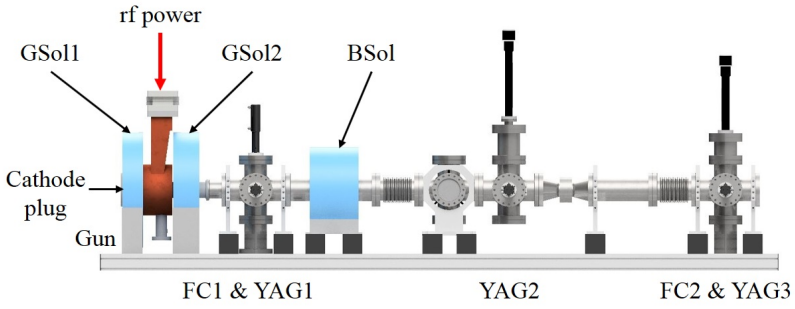


FIG. 2: ACT beamline schematic showing gun solenoids, coincident elements Faraday cup 1 (FC1) and imaging screen (YAG1), beam solenoid (BSol), a second imaging screen (YAG2), coincident elements Faraday cup 2 (FC2) and imaging screen (YAG3).

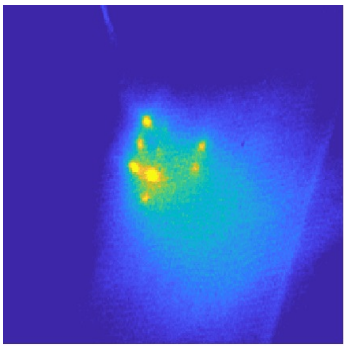

FIG. 3: An image of 9 beamlets on YAG1 at the cathode gradient of 14.9 MV/m.

vantages.

This paper reports the results of the recent experiment that demonstrated shaped beam production from a DFEA cathode in the 1.3 GHz rf gun at the Argonne Cathode Test-stand (ACT) at Argonne National Laboratory [19,20,21]. The DFEA reported on here is a square array of 25 pyramid emitters arranged in a 5x5 pattern with 25 micron base and 400 micron pitch. This cathode sample was chosen specifically to allow for imaging of individual emitted beamlets to most easily observe an emission pattern and determine the spacing between beamlets. Electron beams were produced from this cathode at gradients varying between 12 and 22 MV/m. Out of the 25 emitters, approximately 8 emitters were active at any given time. The bunch charge was measured via Faraday cup, and beam images were observed on several yttrium-aluminium-garnet (YAG) screens along the beamline. The beamlets were transported along the beamline over a distance of more than 2.54 meters, long enough for insertion into an accelerator and the EEX.

A schematic of the ACT is shown in Fig. 2. At the front of the test stand is an L-band normal-conducting high gradient single-cell rf gun. The beamline includes the following components: three YAG screens at various distances from the gun exit (YAG1 at 0.43 m, YAG2 at 1.57 m, and YAG3 at 2.54 m) two Faraday cups (FC1 and FC2 coincident with YAG1 and YAG3, respectively), gun solenoids (GSol1, GSol2), and a beamline solenoid (BSol). Vacuum pressure in the system was $5 \times 10^{-9}$ torr during the experiment. The rf pulse length was 6 $\mu$s with a repetition rate of 2 Hz.

During the experiment, the gradient on the cathode was adjusted by changing the rf power coupled into the gun. Simulations of the cavity determine the field at the cathode based on the input rf power. We start with a low cathode gradient and increase the field until there is an image on the first YAG screen. This is not necessarily the threshold for emission, due to the inherent noise of the measurement system. We then determine if the emission level is above the noise threshold on the Faraday cup.

The image of nine beamlets on YAG1 at 14.9 MV/m is shown in Fig. 3. Some of the glow around the beamlets in the image is due to emission from the edge of the cathode disk and some is due to the wide energy spread of the emission current itself. The beam was ballistically transported further by adjusting the beamline solenoid, BSol, to focus the beamlets onto YAG2 and finally onto YAG3. Bsol was optimized at a field of 365 Gauss. Fig. 4 shows the beam at 15.1 MV/m as it was transported through the beamline. Use of the solenoid, Bsol, also eliminated extraneous emission from the cathode edge, which was verified by beam images on YAG2 and YAG3. The beam was rotated by the magnetic field of BSol, between YAG1 and YAG2. No focusing elements were used between YAG2 and YAG3. The beamlets brightness varied significantly for different emitting tips, thus the

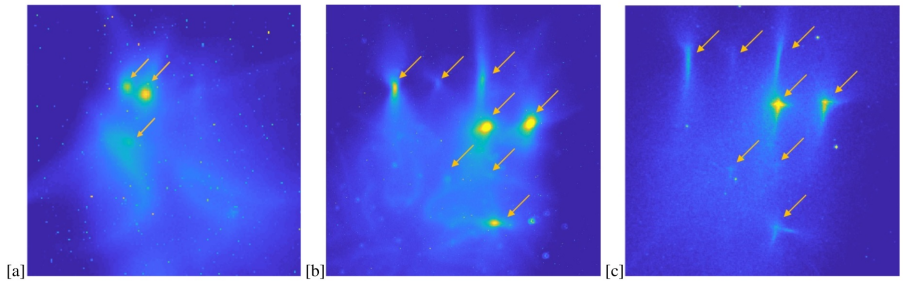


FIG. 4: Image of 3 beamlets on YAG1 at 15.1 MV/m [a]; images of 8 beamlets on YAG2 after Bsol solenoid optimization [b]; and same 8 beamlets transported on to YAG3 [c].

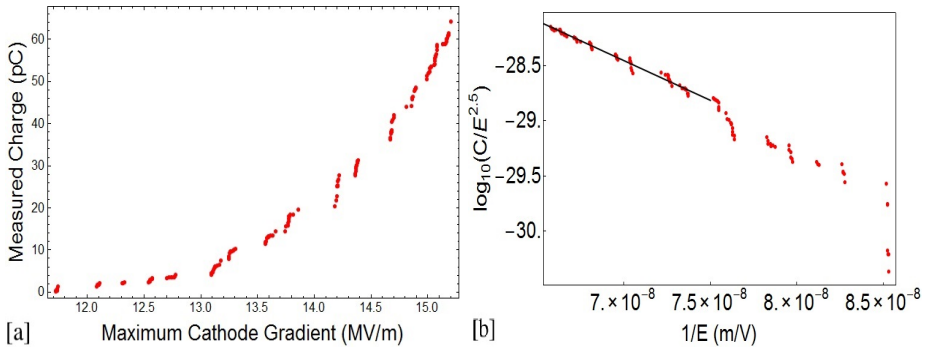


FIG. 5: Bunch charge measured on FC2 at different cathode gradients [a]; the same data from [a] plotted in FN coordinates [b].

average current per tip is a low estimate of what high performing tips were likely contributing. All tips were determined to be sharp by SEM imaging.

Bunch charge was measured with FC1 and FC2, we report charge collected on FC2 here for its accuracy. The maximum bunch charge measured from this array was 60 pC. This particular rf gun was designed to provide 1-100 nC bunch charge between 30 MV/m and 100 MV/m with a photocathode[21,22]. The bunch charge we measured is extremely high for this gun considering the very small emission area of the eight tips. Using the bunch charge measured on FC2 and derived parameters we estimate average per-tip current, maximum average per-tip current, peak current, and per-tip emission area. Bunch charge, measured consecutively at decreasing cathode gradients on FC2, is plotted in Fig. 5[a]. Previous testing has shown that the tips have a breakdown limit above 15 MV/m gradient; 15.1 MV/m was determined to be a gradient at which we could operate for an extended time without incurring cathode damage. Figure 5[b] shows bunch charge versus gradient plotted in Fowler-Nordheim (FN) coordinates[23]. We use the linear portion of this data, the black line in Fig. 5[b], to fit $\beta$, the field enhancement factor at the tips, and $A_e$, the effective emission area. Assuming $\beta$ is constant, it can be determined from[24]:

$$\beta = \frac{-2.84 \times 10^9 \phi^{1.5}}{s} \approx 450. \quad (1)$$

Here $\phi$ is the work function measured by Kelvin probe to be 4.9 eV, and $s$ is the slope of the fitted line. This very high field enhancement factor corresponds to exceptionally sharp emitter tips. Likewise, we determine the effective emission area $A_e$ using[24]:

$$A_e = \frac{10^{y_0} \phi^{1.75}}{5.7 \times 10^{-12} \times 10^{4.52\phi^{-0.5}} \beta} \approx 5490\ nm^2, \quad (2)$$

where $y_0$ is the y-intercept of the fitted line.

We estimate the average per-tip current using our bunch charge measurements of 60 pC at 15.1 MV/m field and the number of observed emitting tips, 8. We find the average per-tip charge per macro-pulse to be 7.5 pC. Dividing this charge by the flat-top macro-pulse duration of 6 $\mu$s, we compute the average current emitted per macro-pulse to be approximately 1.25 $\mu$A per tip. This is a significantly low estimate because

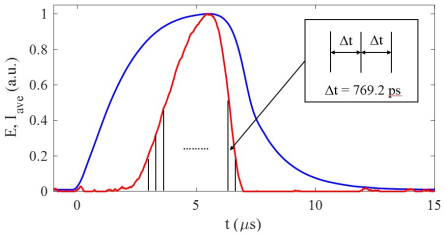


FIG. 6: The blue (solid) curve is the measured rf power in the gun during one 6$\mu$s macro-pulse, the red (dashed) curve is the derived FN emission envelope based on the fitted emission properties and Fig. 5[b]. The black lines represent short bursts of emission current from each 769.2 ps micro-pulse.

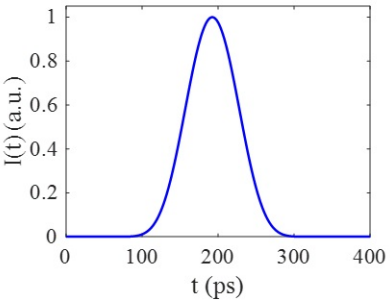


FIG. 7: The temporal shape of the micro-pulse current from Eq.(3) for the micro-pulse occurring at the peak of the red emission curve in Fig. 6.

the tips only emit and current only transports out of the gun for a small fraction of the macro-pulse. We also estimate the maximum average per-tip current by using the enhanced field-emission model[23], which allows us to approximate the maximum current in the derived emission envelope. Equation (10) from Ref.[23] gives us the field-emission current, $I_F$, in Amps, resulting from our effective emitting area:

$$I_F(t) = \frac{1.54\times10^{-6}\times10^{4.52\phi^{-0.5}}A_e\beta^2E_c(t)^2}{\phi} \times exp\left(-\frac{6.53\times10^9\phi^{1.5}}{\beta E_c(t)}\right), \quad (3)$$

where $E(t)$ is the experimentally fitted local electric field at the pyramid tips. This field has a maximum of 6.8 GV/m. Figure 6 illustrates the time structure of the field-emission current. The blue curve is the normalized amplitude of the rf field at the cathode measured inside the gun cavity using an rf pickup. The red curve is the normalized FN emission envelope plotted using Eq.(3), with the area under the curve corresponding to the total charge measured on the Faraday Cup. The black lines represent the bursts of emission current induced by rf micro-pulses. Using the maximum $E(t)$ in Eq.(3) we determine the maximum average emission current to be 2.9 $\mu$A per emitter. This value corresponds to the peak value of the red curve in Fig. 6. This estimated per tip current gives us a baseline measurement for understanding the single tip emission to inform dense array experiments which are complicated by emission suppression due to the electric field on nearby tips.

We further estimate the peak micro-pulse current by multiplying the maximum average current found above by the duration of the rf period to determine the charge in the single peak micro-pulse: $2.9\ \mu A\times769.2\ ps = 2.23\ fC$. We then use Eq.(3), this time using the sinusoidal rf micro-pulse for $E(t)$, and plot the normalized current in Fig 7. The micro-pulse charge is the the integral of the current over the time duration, allowing us to determine the peak micro-pulse current to be 29.4 $\mu A$, similar to the analysis in Ref.[25].

Finally, we estimate the emission area of each emitting pyramid. First, we take the effective emission area of the array, 5490 $nm^2$ and divide it by the eight emitting tips observed in a corresponding YAG image. Taking the square root of this number, we find that each tip was emitting from an area approximately 26 $nm^2$. This dimension corresponds to the very sharp tip of the pyramid, indicating that only very tips of the pyramids are emitting, a long standing hypothesis.

In conclusion, we have demonstrated patterned beam production in an rf gun and transport of the beam over 2.54 m while maintaining the initial pattern of the array. The beam was produced by a DFEA cathode with 25 pyramids in a 1.3 GHz rf gun. Initial experiments show very promising results for the DFEA cathodes: we demonstrated high per-tip current and the ability to maintain the shape (or pattern), of the initial beam during transport. These results show strong potential for DFEAs in other patterns to produce intrinsically shaped beams. Further experimentation on different array geometries is in progress.

The authors gratefully acknowledge the support of Los Alamos National Laboratory (LANL) Laboratory Directed Research and Development (LDRD) program. This work was performed, in part, at the Center for Integrated Nanotechnologies, an Office of Science User Facility operated for the U.S. Department of Energy (DOE) Office of Science by Los Alamos National Laboratory (Contract DE-AC52-06NA25396) and Sandia National Laboratories (Contract DE-NA-0003525). The work at AWA is funded through the U.S. Department of Energy Office of Science under Contract No. DE-AC02-06CH11357. Use of the Center for Nanoscale Materials, an Office of Science user facility, was supported by the U.S. Department of Energy, Office of Science, Office of Basic Energy Sciences, under Contract No. DE-AC02-06CH11357.

[1]W. Gai, P. Schoessow, B. Cole, R. Konecny, J. Norem, J. Rosenzweig, and

J. Simpson, "Experimental demonstration of wake-field effects in dielectric structures," Phys. Rev. Lett. **61**, 2756 (1988).
[2]M. Rosing and W. Gai, "Longitudinal- and transverse-wake-field effects in dielectric structures," Phys. Rev. D **42**, 1829 (1990).
[3]P. Chen, J. M. Dawson, R. W. Huff, and T. Katsouleas, "Acceleration of electrons by the interaction of a bunched electron beam with a plasma," Phys. Rev. Lett. **54**, 693 (1985).
[4]C. Jing, J. G. Power, M. Conde, W. Liu, Z. Yusof, A. Kanareykin, and W. Gai, "Increasing the transformer ratio at the argonne wakefield accelerator," Phys. Rev. Lett. **98**, 144801 (2007).
[5]A. Zholents, W. Gai, S. Doran, R. Lindberg, J. G. Power, N. Strelnikov, Y. Sun, E. Trakhtenberg, I. Vasserman, C. Jing, A. Kanareykin, Y. Li, Q. Gao, D. Y. Shchegolkov, and E. I. Simakov, "A preliminary design of the collinear dielectric wakefield accelerator," Nucl. Instrum. Methods Phys. Res. A **829**, 190 (2016).
[6]F. Lemery and P. Piot, "Tailored electron bunches with smooth current profiles for enhanced transformer ratios in beam-driven acceleration," Phys. Rev. STAB **18**, 081301 (2015).
[7]D. Y. Shchegolkov and E. I. Simakov, "Design of an emittance exchanger for production of special shapes of the electron beam current," Phys. Rev. STAB **17**, 041301 (2014).
[8]G. Ha, M. Cho, W. Namkung, J. G. Power, D. S. Doran, E. E. Wisniewski, M. Conde, W. Gai, W. Liu, C. Whiteford, Q. Gao, K. J. Kim, A. Zholents, Y. E. Sun, C. Jing, and P. Piot, "Precision control of the electron longitudinal bunch shape using an emittance-exchange beam line," Phys. Rev. Lett. **118**, 104801 (2017).
[9]G. Ha, M. Cho, W. Gai, K. Kim, W. Namkung, and J. Power, "Perturbation-minimized triangular bunch for high-transformer ratio using a double dog-leg emittance exchange beam line," Phys. Rev. AB **19**, 121301 (2016).
[10]J. Shao, S. P. Antipov, S. V. Baryshev, H. Chen, M. Conde, W. Gai, G. Ha, C. Jing, J. Shi, F. Wang, and E. Wisniewski, "Observation of high transformer ratio of shaped bunch generated by an emittance-exchange beam line," Phys. Rev. Lett. **120**, 114801 (2018).
[11]A. Halavanau, Q. Gao, , M. Conde, G. Ha, P. Piot, J. G. Power, and E. Wisniewski, "Tailoring of an electron-bunch current distribution via space-to-time mapping of a transversely-shaped photoemission-laser pulse," Phys. Rev. AB **22**, 114401 (2019).
[12]J. Zhao, D. Gamzina, N. Li, J. Li, A. G. Spear, L. Barnett, M. Banducci, S. Risbud, and N. C. L. Jr., "Scandate dispenser cathode fabrication to a high-aspect-ratio high-current-density sheet beam electron gun," IEEE Trans. Electron Devices **59**, 1792 (2012).
[13]A. Halavanau, G. Quing, G. Ha, E. Wisniewski, J. G. Power, and W. Gai, "Spatial control of photoemitted electron beams using a microlens-array transverse-shaping technique," Phys. Rev. AB **20**, 103404 (2017).
[14]K. E. Nichols, H. L. Andrews, D. Y. Shchegolkov, and E. I. Simakov, "Modeling of diamond field emitter arrays for shaped electron beam production," IPAC18 Conf. Proc. **https://doi.org/10.18429/JACoW-IPAC2018-THPML010** (2018).
[15]K. E. Nichols, H. L. Andrews, D. Kim, E. I. Simakov, S. Antipov, G. Chen, M. E. Conde, D. S. Doran, G. Ha, W. Liu, J. F. Power, J. H. Shao, C. Whiteford, and E. E. Wisniewski, "Experimental results of dense array diamond field emitters in rf gun," IPAC19 Conf. Proc. **TUPTS090** (2019).
[16]H. L. Andrews, B. K. Choi, R. L. Fleming, D. Kim, J. W. Lewellen, K. E. Nichols, D. Y. Shchegolkov, and E. I. Simakov, "An investigation of electron beam divergence from a single dfea emitter tip," IPAC18 Conf. Proc. **https://doi.org/10.18429/JACoW-IPAC2018-THPML007** (2018).
[17]J. D. Jarvis, H. L. Andrews, C. A. Brau, B. K. Choi, J. Davidson, W. P. Kang, and Y.-M. Wong, "Uniformity conditioning of diamond field emitter arrays," J. Vac. Sci. Technol. B: Microelectron. Nanometer Struct. Process. Meas. Phenom. **27**, 2264 (2009).
[18]J. W. Lewellen and J. Noonan, "Field-emission cathode gating for rf electron guns," Phys. Rev. STAB **8**, 033502 (2005).
[19]J. Shao, M. Schneider, G. Chen, T. Nikhar, K. Kumar Kovi, L. Spentzouris, E. Wisniewski, J. Power, M. Conde, W. Liu, and S. Baryshev, "High power conditioning and benchmarking of planar nitrogen-incorporated ultrananocrystalline diamond field emission electron source," Phys. Rev. AB. **22**, 123402 (2019).
[20]T. Rao and D. Dowell, *An Engineering Guide to Photoinjectors* (Triveni Rao, David H. Dowell, 2013).
[21]W. Gai, X. Li, J. Power, and P. Schoessow, "Design of a high charge (10-100 nc) and short pulse (2-5 ps) rf photocathode gun for wakefield acceleration," AIP Conf. Proc. **472**, 901 (1999).
[22]J. Power, M. Conde, W. Gai, F. Gao, R. Konecny, W. Liu, and Z. Yusof, "Pepper-pot based emittance measurement of the awa photoinjector," PAC07 Proc. **FRPMN117** (2007).
[23]J. W. Wang and G. A. Loew, "Field-emission and rf breakdown in high-gradient room-tempera linac structures," SLAC Pub. **7684** (1997).
[24]J. Shao, J. Shi, S. P. Antipov, S. V. Baryshev, H. Chen, M. Conde, W. Gai, G. Ha, C. Jing, J. Shi, F. Wang, and E. Wisniewski, "In situ observation of dark current emission in a high gradient rf photocathode gun," Phys. Rev. Lett. **117**, 084801 (2016).
[25]H. Huang, D. Filippetto, C. Papadopoulos, H. Qian, F. Sannibale, and M. Zolotorev, "Longitudinal- and transverse-wake-field effects in dielectric structures," Phys. Rev. STAB **18**, 013401 (2015).
[26]K. Floettmann, "A space charge tracking algorithm astra," http://www.desy.de/ mpyflo/.

PLEASE CITE THIS ARTICLE AS DOI: 10.1063/1.5128109

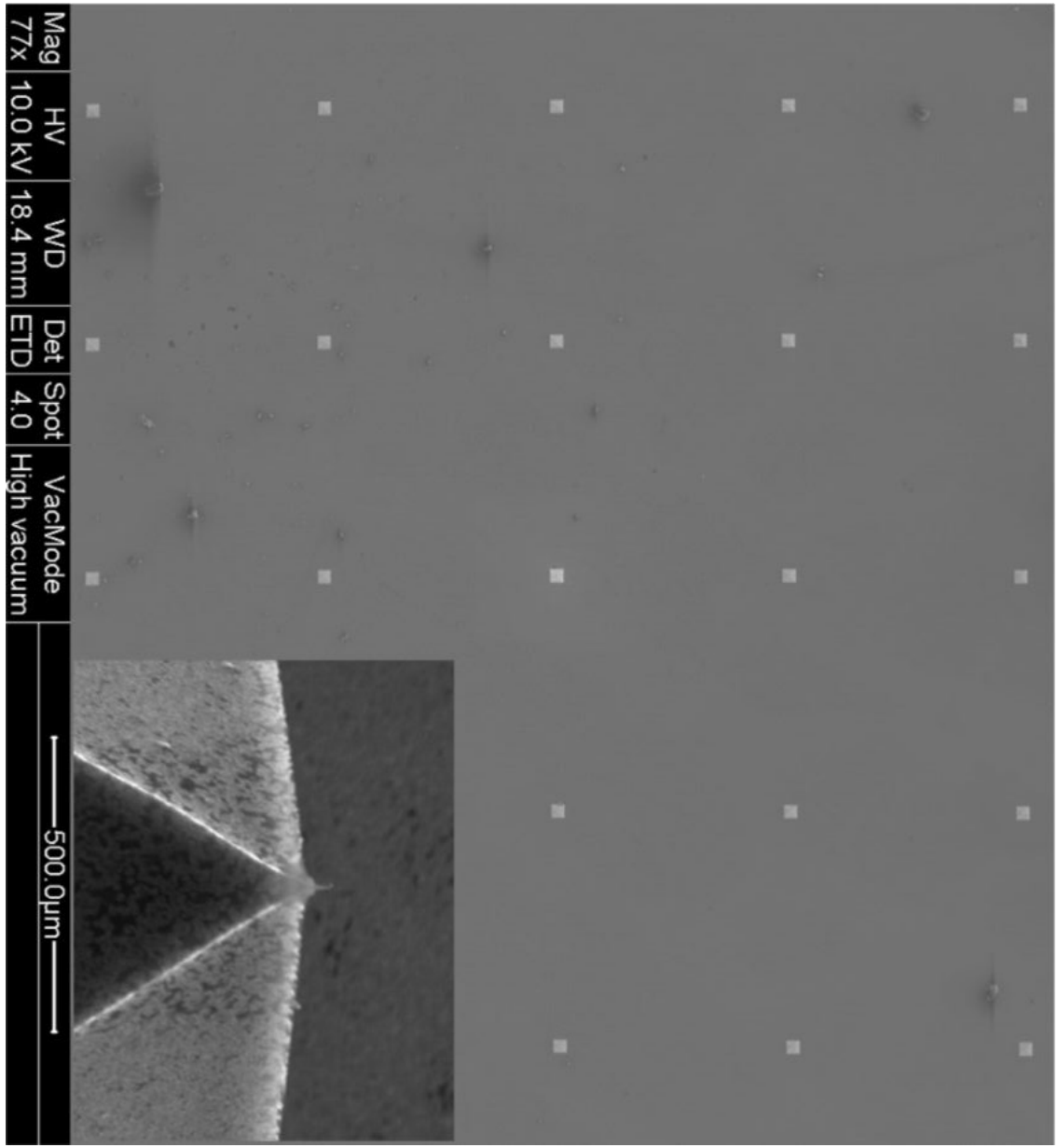

PLEASE CITE THIS ARTICLE AS DOI: 10.1063/1.5128109

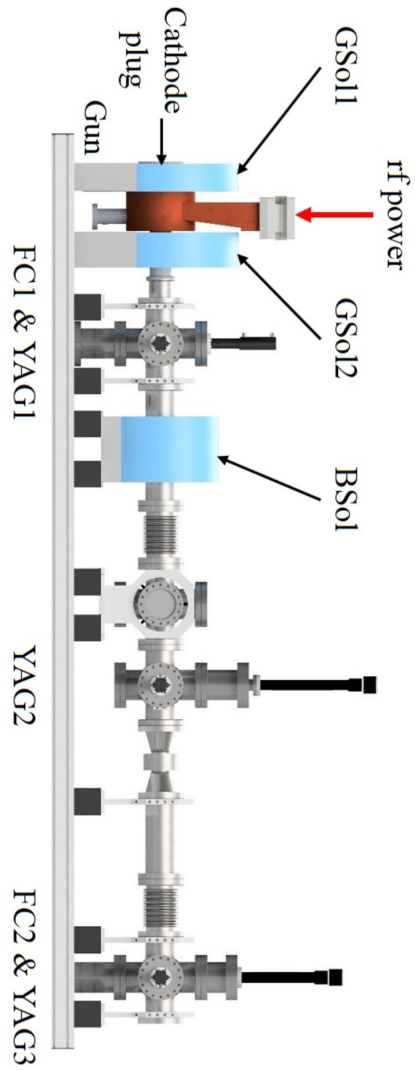

PLEASE CITE THIS ARTICLE AS DOI: 10.1063/1.5128109

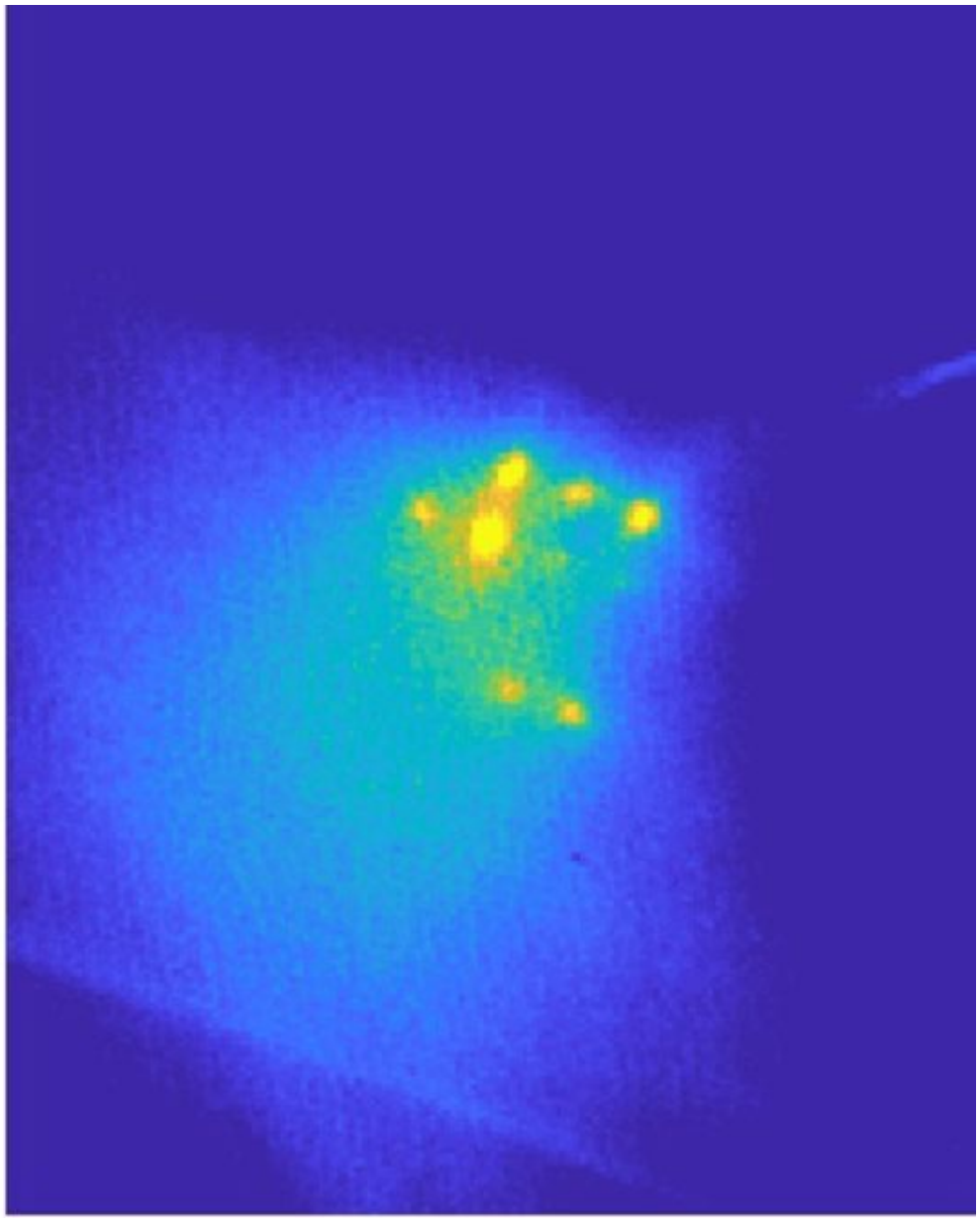

PLEASE CITE THIS ARTICLE AS DOI: 10.1063/1.5128109

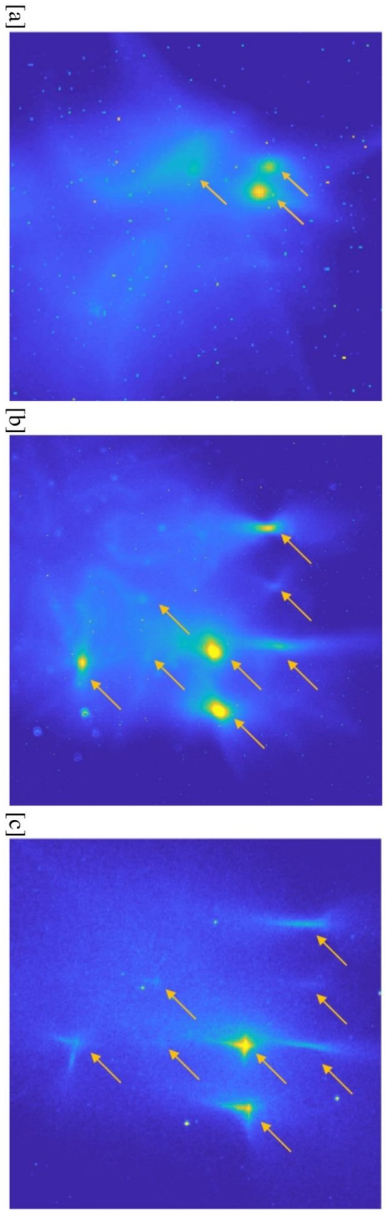

PLEASE CITE THIS ARTICLE AS DOI: 10.1063/1.5128109

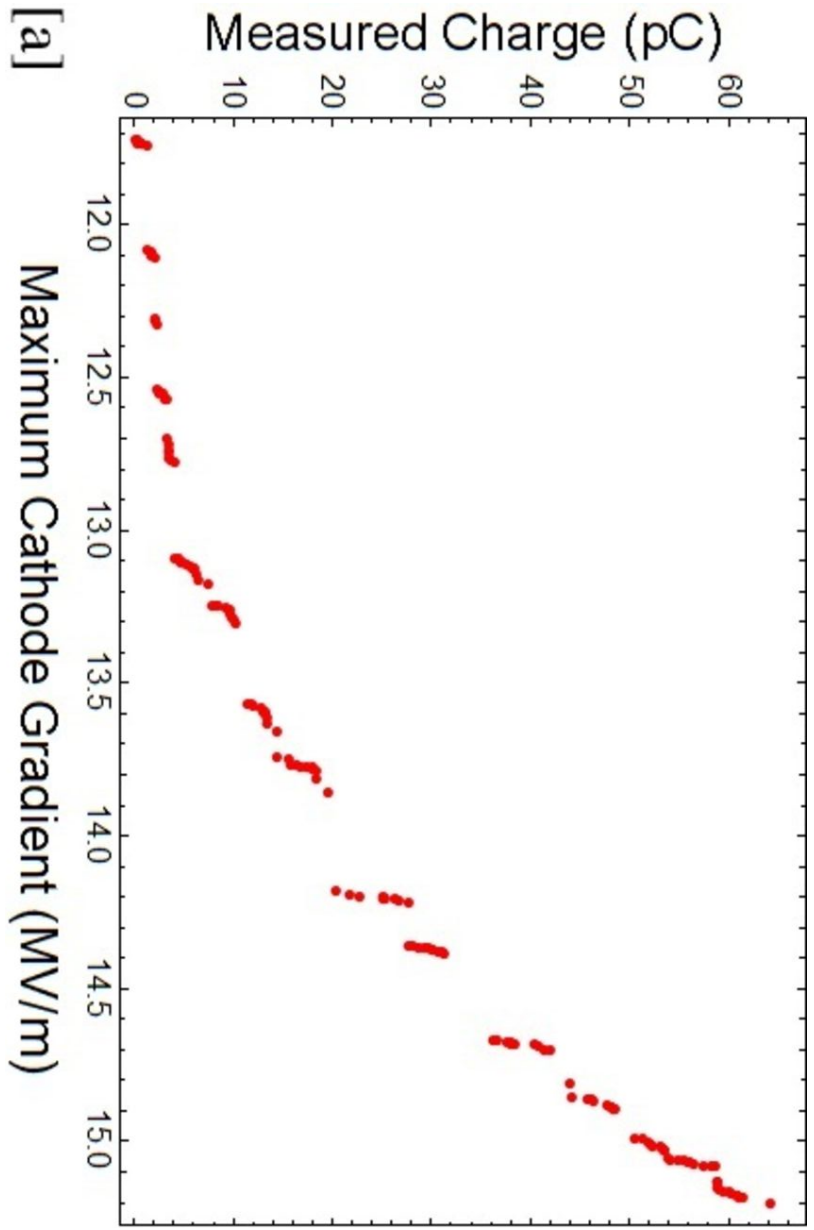

PLEASE CITE THIS ARTICLE AS DOI: 10.1063/1.5128109

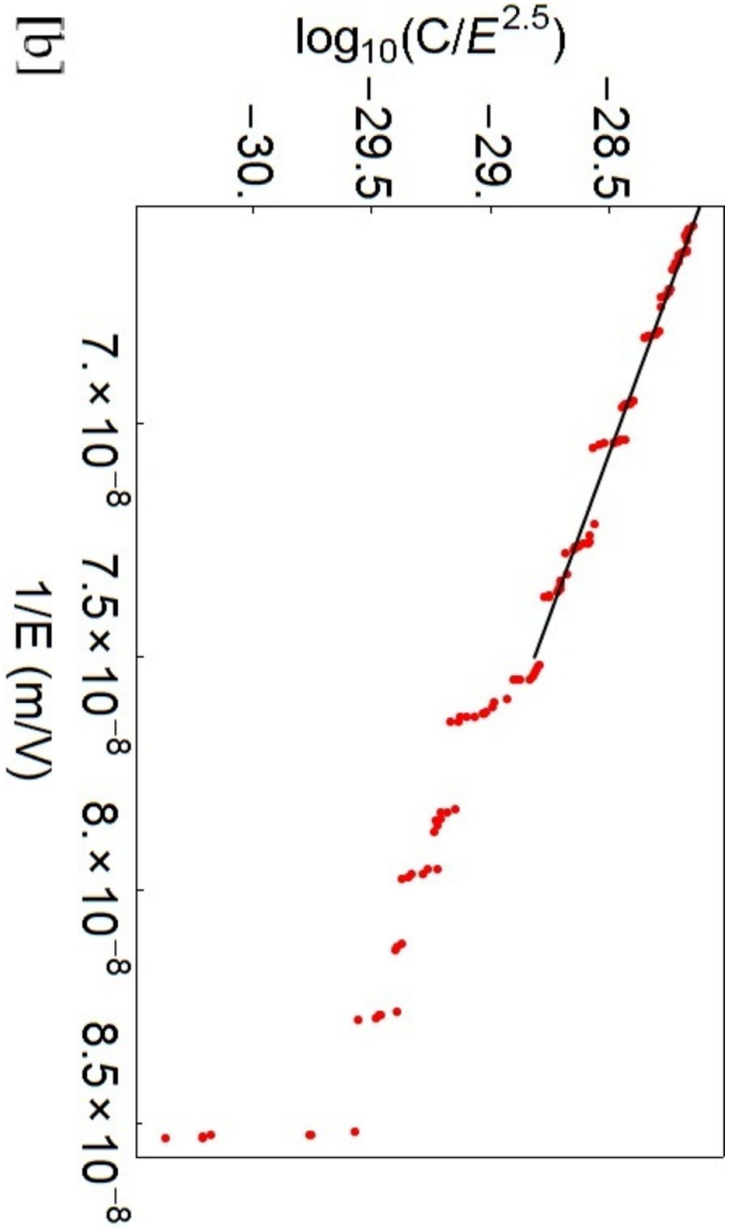

PLEASE CITE THIS ARTICLE AS DOI: 10.1063/1.5128109

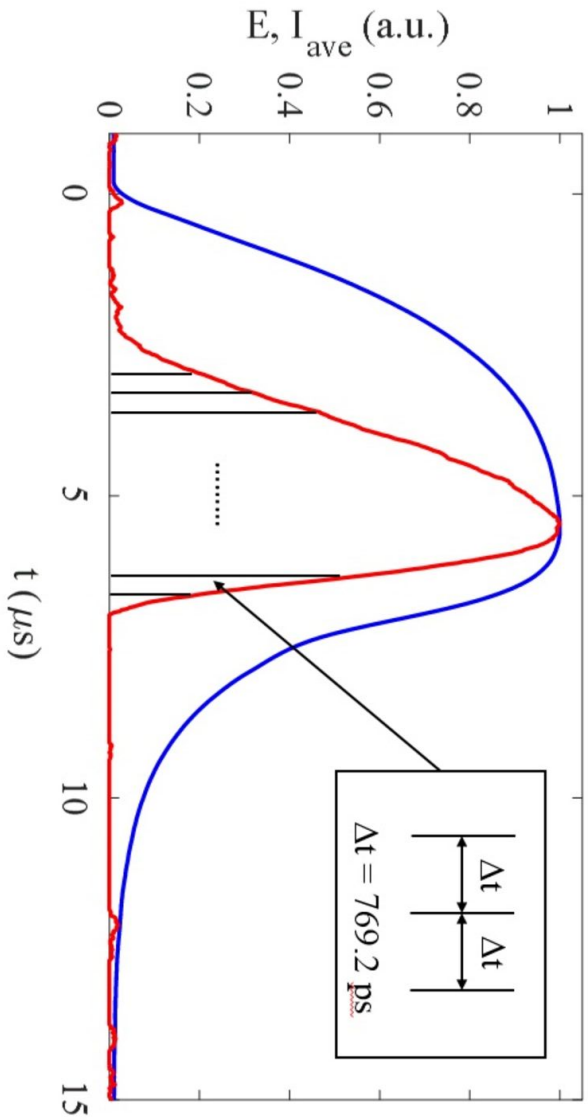

PLEASE CITE THIS ARTICLE AS DOI: 10.1063/1.5128109